Experimental Determination of $\mathcal{PT}$-Symmetric Exceptional Points in a Single Trapped Ion

Liangyu Ding,[1] Kaiye Shi,[1] Qiuxin Zhang,[1] Danna Shen,[1] Xiang Zhang,[1,2,*] and Wei Zhang[1,2,†]
[1]Department of Physics, Renmin University of China, Beijing 100872, China
[2]Beijing Key Laboratory of Opto-electronic Functional Materials and Micro-nano Devices, Renmin University of China, Beijing 100872, China

(Received 28 October 2020; accepted 3 February 2021; published 23 February 2021)

Exceptional points (EPs) of a non-Hermitian Hamiltonian with parity-time-reversal ($\mathcal{PT}$) symmetry have the potential to drastically enhance the capabilities of metrology and sensing through their power-law growing sensitivity to external perturbation. With the ability of generating and tuning dissipation in a single trapped ion system, we observe rich dynamics and detailed quantum phase transitions from the $\mathcal{PT}$-symmetric phase to the symmetry-breaking phase. In this single qubit full quantum system, we develop a method to precisely determine the location of EP without any fitting parameter, and extract the eigenvalues in a unified way through all parameter regions. We can also obtain the full density matrix by quantum state tomography. Finally, we suggest from theoretical analysis that the periodically driving $\mathcal{PT}$-symmetric non-Hermitian system can be used to measure the magnitude, frequency, and phase of time-dependent perturbation with EP enhancement.

DOI: 10.1103/PhysRevLett.126.083604

Introduction.—A non-Hermitian Hamiltonian with parity-time-reversal ($\mathcal{PT}$) symmetry, whose spectra is also real in some regime, is generally regarded as a natural extension of conventional quantum theories from real phase space to complex phase space [1]. An unconventional phase transition occurs across an extraordinary type of singular point called an exceptional point (EP), at which the real spectra transits to complex conjugate pairs and the $\mathcal{PT}$ symmetry is spontaneously broken [2,3]. These EPs have the potential to drastically enhance the capability of metrology and sensing through their power-law growing sensitivity to external perturbation [4,5].

By manipulating the gains and losses in exchange with an environment, many experimental works have been performed to explore static and dynamical characteristics near EPs. The $\mathcal{PT}$-symmetric non-Hermitian Hamiltonian were generally implemented in quasiclassical systems with balanced gain and loss, such as cavities [6–8], electronics [9–14], photonics [15,16], acoustic-mechanical systems [17,18], nonlinear medium [19–23], acoustic resonators [24,25], and single-mode lasers [26,27], where only the amplitude information was measured. Recent progress has also included more challenging approaches in mapped open quantum systems [28], such as the optical pure lossy system [29], single-photon interferometric network [30,31], cold atoms [32,33], nitrogen-vacancy centers [34,35], superconducting circuits [36,37], entangled photons [38] and trapped ions [39], where the quantum phase information could be obtained in principle.

In order to achieve the EP enhancement of quantum metrology and sensing, it is crucial to accurately determine the location of EPs in experiments and measure the asymptotic behavior of the energy around the EP without special prior knowledge. This is in general a difficult task for quantum systems and has not been reported in any previous work, mainly owing to the lack of feasible method to precisely measure the eigenvalues of non-Hermitian systems. Here, we develop a novel protocol inspired by quantum state tomography [40], and directly determine the eigenvalues and EPs without any fitting parameter. We first realize various $\mathcal{PT}$-symmetric non-Hermitian Hamiltonians using four Zeeman levels of a single trapped Yb^+ ion through state-dependent dissipative processes. $\mathcal{PT}$-symmetry breaking phenomena and quantum phase transition dynamics across the EP are experimentally observed. Our work is the first experimental scheme to simultaneously generate and fine-tune dissipation and interlevel interaction with arbitrary time dependence in a massive single qubit system. To show the capability of this scheme, we realize a Floquet non-Hermitian system under periodic driving, and map out the phase diagram without any fitting parameter. Finally, we demonstrate by theoretical analysis that the system can be employed as a quantum sensor to extract the magnitude, frequency, and phase of an external time-dependent perturbation.

Experimental system.—We consider a single qubit non-Hermitian Hamiltonian with $\mathcal{PT}$ symmetry

$$\hat{H}_{\mathcal{PT}} = J\hat{\sigma}_x + i\Gamma\hat{\sigma}_z, \tag{1}$$

where $\hat{\sigma}_x \equiv |\downarrow\rangle\langle\uparrow| + |\uparrow\rangle\langle\downarrow|$ and $\hat{\sigma}_z \equiv |\downarrow\rangle\langle\downarrow| - |\uparrow\rangle\langle\uparrow|$ are Pauli operators. The time evolution of a quantum state $|\psi(t)\rangle$ satisfies the Schrödinger type equation

$$i\frac{d}{dt}|\psi(t)\rangle = \hat{H}_{\mathcal{PT}}|\psi(t)\rangle. \quad (2)$$

The state $|\psi(t)\rangle$ can be mapped to another state $|\Psi(t)\rangle = e^{-\Gamma t}|\psi(t)\rangle$, whose evolution is governed by a mapped Hamiltonian

$$\hat{H}'_{\mathcal{PT}} = \hat{H}_{\mathcal{PT}} - i\Gamma\hat{I}, \quad (3)$$

with $\hat{I} = |\downarrow\rangle\langle\downarrow| + |\uparrow\rangle\langle\uparrow|$ the identity operator. Thus, if one can realize the mapped $\hat{H}'_{\mathcal{PT}}$, the evolution of the original $\mathcal{PT}$-symmetric Hamiltonian $\hat{H}_{\mathcal{PT}}$ can be obtained by measuring the mapped state $|\Psi(t)\rangle$ and removing the scaling factor $e^{-\Gamma t}$.

In our experiment, the mapped Hamiltonian $\hat{H}'_{\mathcal{PT}}$ is realized in a dissipative single qubit system, where the spin states $|\downarrow\rangle$ and $|\uparrow\rangle$ correspond, respectively, to the two hyperfine states $|F = 0, m = 0\rangle$ and $|F = 1, m = 0\rangle$ in the $^2S_{1/2}$ ground level manifold of $^{171}Yb^+$, with a hyperfine splitting $\omega_{HF} \approx 12.6$ GHz. We use microwave to couple this interlevel transition and the coupling strength J is measured by fitting the Rabi frequency. A weak 369.5 nm beam is used to excite the ion from $|F = 1, m = 0\rangle$ to the upper $^2P_{1/2}$ state, and the beam contains only π-polarization components to ensure that excitations from any other Zeeman states ($|F = 1, m = \pm 1\rangle$) are forbidden by selection rules. The excited $^2P_{1/2}$ state can spontaneously decay to all three Zeeman states of the $^2S_{1/2}$ manifold by emitting photons with $\sigma_\pm$ or π polarizations, resulting in a loss of $|\uparrow\rangle$ state at a dissipation rate 4Γ. The experimental setup and a diagram of this scheme are illustrated in Fig. 1(a). A more detailed description of the experimental system and a theoretical derivation of this dissipative scheme using the Lindblad master equation can be found in Supplemental Material [41].

The population of the $|\downarrow\rangle$ state is directly measured by the standard fluorescence counting rate threshold method [42], which is described in Supplemental Material [41]. The other state $|\uparrow\rangle$ is measured by adding appropriate π flips. With the results of $|\uparrow\rangle$ state population, we can obtain the dissipation rate Γ from a fitting of exponential decay by turning on the 369.5 nm dissipative beam only. A typical set of data is shown in Fig. 1(b). The mapped Hamiltonian $\hat{H}'_{\mathcal{PT}}$ is realized by applying the coupling ω_{HF} and dissipative beams simultaneously, where a clear combination of exponential decay and Rabi oscillation is observed as in Fig. 1(c). In this plot, we prepare the system in the initial state $|\downarrow\rangle$, a detection of the same state $|\downarrow\rangle$ after a certain time evolution is given by

$$|\langle\downarrow|\exp(-i\hat{H}'_{\mathcal{PT}}t)|\downarrow\rangle|^2 = e^{-2\Gamma t}\left[\cos(\epsilon t) + \frac{\Gamma}{\epsilon}\sin(\epsilon t)\right]^2, \quad (4)$$

where $\epsilon \equiv \sqrt{J^2 - \Gamma^2}$. We can also obtain the parameters J and Γ from a fitting of the expression above. The results are

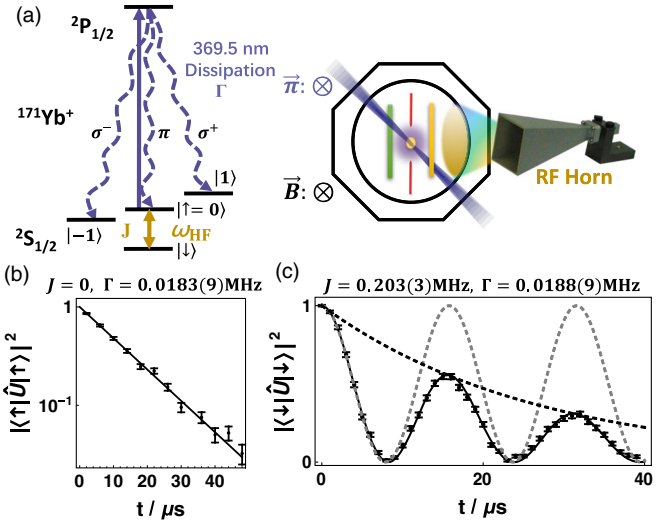

FIG. 1. (a) The energy level of $^{171}Yb^+$ and the experimental setup. (b) Time evolution of the $|\uparrow\rangle$ state population without interspin coupling. The dissipation rate Γ is determined by an exponential fit. (c) Evolution of the $|\uparrow\rangle$ state population with both the coupling and dissipation beams. The data can be fit by a combination of a Rabi oscillation (gray dashed) and an exponential decay (black dashed). The evolution operator is defined as $\hat{U} = e^{-i\hat{H}'_{\mathcal{PT}}t}$. For panels (b) and (c), the black solid curve is the numerical simulation and the points are experimental data averaged from 1000 rounds of measurement. The error bars in J and Γ are estimated by the standard deviation (1σ) of 20 rounds of experiment and fitting [41].

in good agreement with the ones from Rabi frequency and exponential decay alone.

Phase transition.—The dynamical evolution of a Hermitian Hamiltonian can be represented by a unitary operator. For a single qubit, the evolution can always be expressed as a rotation on a Bloch sphere, where the eigenvectors of the Hamiltonian correspond to the rotation axes, and the eigenvalues to the rotating velocities. This property thus allows us to determine the eigenvalues by fitting the Rabi oscillation of the state population. For a $\mathcal{PT}$-symmetric non-Hermitian system, the eigenvalues are also real in the $\mathcal{PT}$-symmetry preserving phase, and the same scheme can be used to measure the eigenvalues. However, in the $\mathcal{PT}$-symmetry broken regime, the eigenvalues acquire imaginary components and can no longer be considered as rotating velocities. Previous works usually employ different schemes to extract the eigenvalues for the two phases, and locate the EP by comparing their individual results.

Here, we introduce an improved method based on quantum state tomography. This method can measure the eigenvalues in a unified scheme within a wide range across the $\mathcal{PT}$ transition, and precisely determine the EP. By evolving from a proper initial state and measuring with a specific basis, we can define the following two quantities:

$$P_J(t) = |\langle\uparrow|\exp(-i\hat{H}_{\mathcal{PT}}t)|\downarrow\rangle|^2 = \frac{J^2}{J^2-\Gamma^2}\sin^2(t\sqrt{J^2-\Gamma^2}),$$
$$P_\Gamma(t) = \left|\frac{\langle\uparrow|-\langle\downarrow|}{\sqrt{2}}\exp(-i\hat{H}_{\mathcal{PT}}t)\frac{|\uparrow\rangle+|\downarrow\rangle}{\sqrt{2}}\right|^2 = \frac{\Gamma^2}{J^2-\Gamma^2}\sin^2(t\sqrt{J^2-\Gamma^2}), \quad (5)$$

which can both be obtained from population measurement of the two spin states and a reverse mapping from $\hat{H}'_{\mathcal{PT}}$ to $\hat{H}_{\mathcal{PT}}$. Further details are discussed in Supplemental Material [41]. By subtracting the two quantities, we find that the sign of $P_J(t) - P_\Gamma(t)$ is positive (negative) in the $\mathcal{PT}$-symmetry unbroken (broken) phase, thus works as an indicator for the phase boundary. The eigenvalues can be obtained as $E = \pm\sqrt{J^2-\Gamma^2}$ (unbroken) or $\pm i\sqrt{\Gamma^2-J^2}$ (broken) by calculating arcsin or arcsinh functions followed by a division over time. Higher accuracy can be achieved by performing an additional linear fit along the scanning time t.

Since an unknown external perturbation may bring a system around an EP to either unbroken or broken regime, the ability of using a unified method to distinguish the two phases and extract the eigenvalues is of particular importance for potential applications in quantum metrology. As a side benefit, the coefficient $J^2/(J^2-\Gamma^2)$ is automatically eliminated, thereby avoiding the unstable multiparameter nonlinear fitting of the exponentially damped Rabi oscillation as shown in Fig. 1(c).

To demonstrate the feasibility of this method, we tune the system to scan the relative ratio of coupling and dissipation J/Γ, while the evolving time is fixed at $t = 1/J$. The EP is determined experimentally by calculating the intersection of two interpolated curves, and agrees well with the theoretical prediction of $J = \Gamma$ as shown in Fig. 2(a). We also obtain the eigenvalues at some typical values of J/Γ in both the unbroken and broken regimes by linear fitting with evolution time, and find good agreement with theoretical predictions as shown in Figs. 2(b) and 2(c).

We then study the full quantum dynamics of the $\mathcal{PT}$-symmetric Hamiltonian and the important phase information by measuring the density matrix $\rho = |\psi_0(t)\rangle\langle\psi_0(t)|$ of nonunitary time evolution, where $|\psi_0(t)\rangle = e^{-i\hat{H}_{\mathcal{PT}}t}|\downarrow\rangle$. The matrix element of the density matrix is $\rho_{|mn\rangle} = \langle m|\rho|n\rangle$. When the eigenvalues are real, the system is in the $\mathcal{PT}$-symmetric phase. The diagonal and off-diagonal elements, which represent, respectively, the state population and quantum coherence, exhibit bounded Rabi oscillations as shown in Fig. 2(d). The two eigenvalues approach zero and the corresponding eigenmodes become degenerate at the second-order EP, across which the system transits to the $\mathcal{PT}$-symmetry broken phase [46]. The eigenvalues then become pure imaginary, and all the diagonal and off-diagonal elements of density matrix increase exponentially over time, as shown in Fig. 2(e). Note that only the imaginary part of the off-diagonal elements are depicted since they are always pure imaginary in theory. Using the quantum state tomography technique, we measure the complete quantum state density matrix at two typical choices of J/Γ before and after the EP. From Fig. 2(f), we observe a good agreement between experimental data and theoretical calculations, which demonstrates the reliability of our system and the measuring protocol.

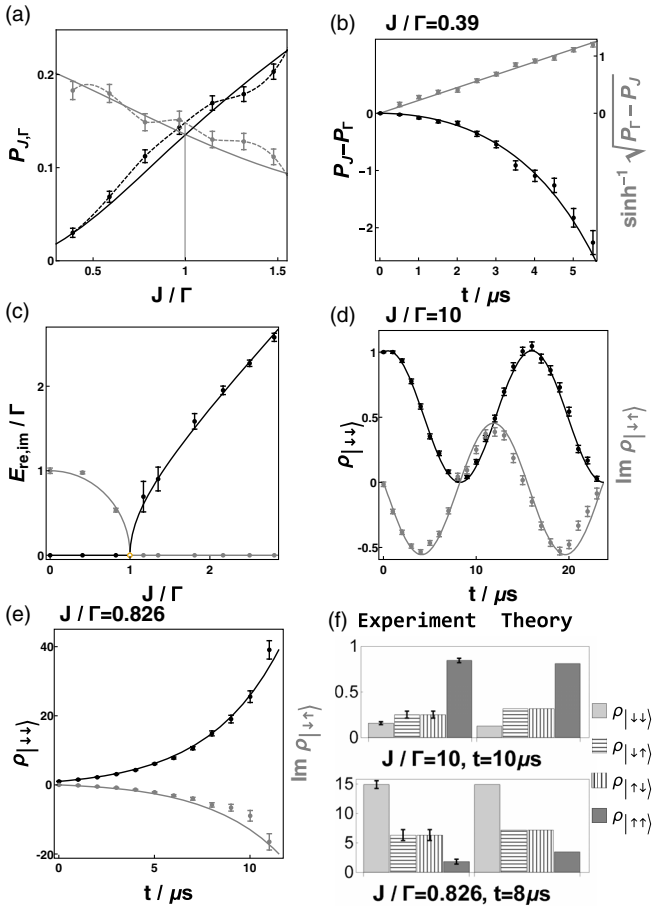

FIG. 2. (a) Determination of EP from the measurement of $P_J(t)$ (black) and $P_\Gamma(t)$ (gray). (b) In the $\mathcal{PT}$-symmetry broken phase, we can calculate from $P_J(t) - P_\Gamma(t)$ (black) the results of $\sinh^{-1}[P_\Gamma(t) - P_J(t)]$ (gray), which show a clear linear time dependence with the slope being one of the eigenvalues. (c) The real (black) and imaginary (gray) parts of the eigenvalues. (d) The upper diagonal (black) and the imaginary part of the off-diagonal (gray) elements of the density matrix ρ obtained in the $\mathcal{PT}$-symmetric phase with $J/\Gamma = 10$. (e) The same results as in (d) for the $\mathcal{PT}$-symmetry broken phase with $J/\Gamma = 0.826$. (f) The upper panel shows absolute values of the density matrix at $t = 10$ μs of (d) and the lower panel shows the same at $t = 8$ μs of (e). The left two plots are measured using quantum state tomography and the right are numerical simulations. For (a)–(e), the solid curves are numerical results and the dashed lines are interpolations.

Floquet system.—We extend the discussion to non-Hermitian $\mathcal{PT}$-symmetric systems under periodic driving, which can host richer phase diagrams [32,47–50]. Previous studies have shown that the symmetry breaking of a Floquet system is related to multiphoton resonance processes [32,48]. Many theoretical works consider the periodic modulation of dissipation rate, and predict infinite resonance peaks as the magnitude of dissipation tends to zero [48–50]. Recently, an experiment with cold atom has extended the discussion to the case of periodically modulating coupling J, and observed similar multiphoton resonance processes but with a quantitative difference [32].

We first study the situation where the interspin coupling oscillates cosinusoidally between $0 \sim 2J$ at a frequency ω, where the instantaneous Hamiltonian reads

$$\hat{H}_{\mathcal{PT}} = J[1 + \cos(\omega t)]\hat{\sigma}_x + i\Gamma\hat{\sigma}_z. \tag{6}$$

Using the Floquet method, we can define an effective Hamiltonian

$$\hat{H}_{\text{eff}} = \frac{i}{T}\log(\mathbb{T}e^{-i\int_0^T \hat{H}_{\mathcal{PT}}dt}), \tag{7}$$

where T is the period of modulation and $\mathbb{T}$ is the time-ordering operator. As proved in Supplemental Material [41], when $\hat{H}_{\mathcal{PT}}$ has even time parity within a period, i.e., $\hat{H}_{\mathcal{PT}}(T/2 - t) = \hat{H}_{\mathcal{PT}}(T/2 + t)$, the effective Hamiltonian $\hat{H}_{\text{eff}}$ is $\mathcal{PT}$ symmetric and takes the form $\hat{H}_{\text{eff}} = J_{\text{eff}}\hat{\sigma}_x + i\Gamma_{\text{eff}}\hat{\sigma}_z$, where the effective parameters J_{eff} and Γ_{eff} depend on the driving frequency ω [41]. A $\mathcal{PT}$ transition can be defined for this effective Floquet Hamiltonian at $J_{\text{eff}}/\Gamma_{\text{eff}} = 1$.

We focus on the case of $J > \Gamma$, where the instantaneous Hamiltonian Eq. (6) is in the $\mathcal{PT}$-symmetric regime in most of the time within an oscillating period. When the driving frequency ω is small, this Floquet system is $\mathcal{PT}$ symmetric with $J_{\text{eff}}/\Gamma_{\text{eff}} > 1$ and the state population presents an oscillatory behavior in time evolution as shown in Fig. 3(a).

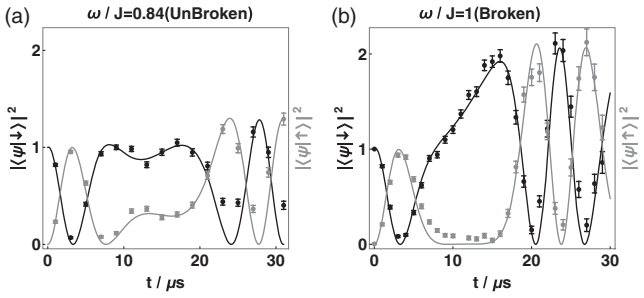

FIG. 3. (a) Evolution of the state population for $|\downarrow\rangle$ (black) and $|\uparrow\rangle$ (gray) for the periodically modulating Hamiltonian equation (6) with $J/\Gamma = 11.11$ and $\omega/J = 0.84$. The effective Floquet Hamiltonian is in the $\mathcal{PT}$-symmetry unbroken phase. (b) Population for the $\mathcal{PT}$-symmetry broken phase with $J/\Gamma = 6.25$ and $\omega/J = 1$. The solid curves are numerical simulations.

By increasing ω beyond a critical value, one can tune the system into the $\mathcal{PT}$-symmetry broken phase, where the oscillation is enhanced as illustrated in Fig. 3(b). Nonetheless, the difference between the two scenarios is much less significant than that for static Hamiltonians, in which case the comparison is made between exponential divergence and bounded oscillation. Thus, one may have to rely on a quantitative analysis of the population measurement to distinguish the two phases. By using our scheme, however, one can obtain the values of P_J and P_Γ from state population at $t = T$ [41], and clearly identify the phase by calculating $P_J - P_\Gamma$ as 0.86 [Fig. 3(a)] and −0.12 [Fig. 3(b)] for the $\mathcal{PT}$-symmetric and broken phases, respectively.

The method can be directly applied to cases with more general time dependency, especially the ones without simple analytic solution. To demonstrate such an ability, we implement a cosinusoidal modulation on the coupling J between $0 \sim 2J$ at frequency ω, and simultaneously a square-wave modulation on the dissipation between $0 \sim \Gamma$ at the same frequency and phase. The time-dependent Hamiltonian is

$$\hat{H}_{\mathcal{PT}} = J[1 + \cos(\omega t)]\hat{\sigma}_x + i\Gamma\frac{1 - \text{sign}[\cos(\omega t)]}{2}\hat{\sigma}_z. \tag{8}$$

In Fig. 4, we determine the phase diagram by measuring $P_J - P_\Gamma$ at time $t = 2\pi/\omega$ (data shown in Supplemental Material [41]) and observe good agreement between experimental results (left) and numerical simulations (right). One can identify four $\mathcal{PT}$-symmetry broken regions, which get narrower with decreasing Γ and eventually merge to points at $\omega/(2J) = 1, 1/2, 1/3$, and $1/4$, respectively. These $\mathcal{PT}$-symmetry broken points at $\Gamma \to 0$ can be explained by multiphoton resonance processes, which are also predicted and observed in a periodically

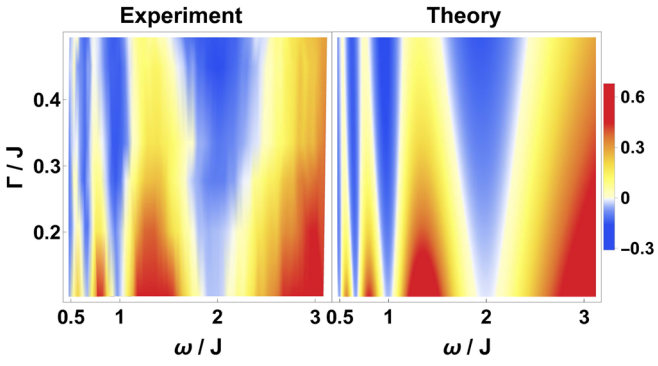

FIG. 4. Phase diagram of the time-dependent Hamiltonian Eq. (8) obtained from measurement of $P_J(t) - P_\Gamma(t)$. The red and yellow regions with positive $P_J(t) - P_\Gamma(t)$ label the $\mathcal{PT}$-symmetric phase, while the blue regions with negative value correspond to the $\mathcal{PT}$-symmetry broken phase. To depict results with different Γ in the same plot, the unscaled data of $P_J(t) - P_\Gamma(t)$ are shown without multiplying the scaling factor.

modulating non-Hermitian system of different forms [32,47–50]. In principle, the same results can also be obtained for higher resonance points. However, the $\mathcal{PT}$-symmetry broken regions become very narrow, such that the phase boundaries are highly sensitive to experimental errors. The ability of precisely determining EPs can be employed in quantum metrology to measure unknown time-dependent signals with EP enhancement. A detailed analysis of this proposal is discussed in Supplemental Material [41].

Summary.—We implement various types of non-Hermitian Hamiltonians in a single trapped ion, and observe rich quantum dynamics to characterize the transition from the $\mathcal{PT}$-symmetry preserving phase to the broken phase in a full quantum bit system. We develop a method to precisely determine the location of exceptional point without any fitting parameter, and to extract the eigenvalues and the full density matrix in a unified way. This protocol works in both static and periodically driving systems, and thus can be employed to measure arbitrary unknown perturbation with EP enhancement. The sensitivity may be further improved by increasing ion numbers [5] or replacing the mapping with actual gain [34].

This work is supported by the National Natural Science Foundation of China (Grants No. 11522436, No. 11774425, No. 11704408, and No. 91836106), the National Key R&D Program of China (Grant No. 2018YFA0306501), the Beijing Natural Science Foundation (Grant No. Z180013), the Joint fund of the Ministry of Education (Grant No. 6141A020333xx), and the Research Funds of Renmin University of China (Grants No. 16XNLQ03 and No. 18XNLQ15).

*siang.zhang@ruc.edu.cn
†wzhangl@ruc.edu.cn

[1] C. M. Bender and S. Boettcher, Phys. Rev. Lett. **80**, 5243 (1998).
[2] T. Kato, *Perturbation Theory for Linear Operators*, 2nd ed., Classics in Mathematics (Springer-Verlag, Berlin, Heidelberg, 1995).
[3] W. D. Heiss, J. Phys. A **37**, 2455 (2004).
[4] H. Hodaei, A. U. Hassan, S. Wittek, H. Garcia-Gracia, R. El-Ganainy, D. N. Christodoulides, and M. Khajavikhan, Nature (London) **548**, 187 (2017).
[5] L. Pan, S. Chen, and X. Cui, Phys. Rev. A **99**, 011601(R) (2019).
[6] C. Dembowski, H.-D. Gräf, H. L. Harney, A. Heine, W. D. Heiss, H. Rehfeld, and A. Richter, Phys. Rev. Lett. **86**, 787 (2001).
[7] S.-B. Lee, J. Yang, S. Moon, S.-Y. Lee, J.-B. Shim, S. W. Kim, J.-H. Lee, and K. An, Phys. Rev. Lett. **103**, 134101 (2009).
[8] B. Peng, S. K. Özdemir, F. Lei, F. Monifi, M. Gianfreda, G. L. Long, S. Fan, F. Nori, C. M. Bender, and L. Yang, Nat. Phys. **10**, 394 (2014).
[9] J. Schindler, A. Li, M. C. Zheng, F. M. Ellis, and T. Kottos, Phys. Rev. A **84**, 040101(R) (2011).
[10] C. E. Rüter, K. G. Makris, R. El-Ganainy, D. N. Christodoulides, M. Segev, and D. Kip, Nat. Phys. **6**, 192 (2010).
[11] L. Feng, M. Ayache, J. Huang, Y.-L. Xu, M.-H. Lu, Y.-F. Chen, Y. Fainman, and A. Scherer, Science **333**, 729 (2011).
[12] S. Bittner, B. Dietz, U. Günther, H. L. Harney, M. Miski-Oglu, A. Richter, and F. Schäfer, Phys. Rev. Lett. **108**, 024101 (2012).
[13] S. Assawaworrarit, X. Yu, and S. Fan, Nature (London) **546**, 387 (2017).
[14] Y. Choi, C. Hahn, J. W. Yoon, and S. H. Song, Nat. Commun. **9**, 2182 (2018).
[15] A. Regensburger, C. Bersch, M.-A. Miri, G. Onishchukov, D. N. Christodoulides, and U. Peschel, Nature (London) **488**, 167 (2012).
[16] B. Zhen, C. W. Hsu, Y. Igarashi, L. Lu, I. Kaminer, A. Pick, S.-L. Chua, J. D. Joannopoulos, and M. Soljačić, Nature (London) **525**, 354 (2015).
[17] C. M. Bender, B. K. Berntson, D. Parker, and E. Samuel, Am. J. Phys. **81**, 173 (2013).
[18] H. Xu, D. Mason, L. Jiang, and J. G. E. Harris, Nature (London) **537**, 80 (2016).
[19] C. Hang, G. Huang, and V. V. Konotop, Phys. Rev. Lett. **110**, 083604 (2013).
[20] P. Peng, W. Cao, C. Shen, W. Qu, J. Wen, L. Jiang, and Y. Xiao, Nat. Phys. **12**, 1139 (2016).
[21] Z. Zhang, Y. Zhang, J. Sheng, L. Yang, M.-A. Miri, D. N. Christodoulides, B. He, Y. Zhang, and M. Xiao, Phys. Rev. Lett. **117**, 123601 (2016).
[22] B.-I. Popa and S. A. Cummer, Nat. Commun. **5**, 3398 (2014).
[23] M. Brandstetter, M. Liertzer, C. Deutsch, P. Klang, J. Schöberl, H. E. Türeci, G. Strasser, K. Unterrainer, and S. Rotter, Nat. Commun. **5**, 4034 (2014).
[24] X. Zhu, H. Ramezani, C. Shi, J. Zhu, and X. Zhang, Phys. Rev. X **4**, 031042 (2014).
[25] R. Fleury, D. Sounas, and A. Alù, Nat. Commun. **6**, 5905 (2015).
[26] H. Hodaei, M.-A. Miri, M. Heinrich, D. N. Christodoulides, and M. Khajavikhan, Science **346**, 975 (2014).
[27] L. Feng, Z. J. Wong, R.-M. Ma, Y. Wang, and X. Zhang, Science **346**, 972 (2014).
[28] J. T. Barreiro, M. Müller, P. Schindler, D. Nigg, T. Monz, M. Chwalla, M. Hennrich, C. F. Roos, P. Zoller, and R. Blatt, Nature (London) **470**, 486 (2011).
[29] A. Guo, G. J. Salamo, D. Duchesne, R. Morandotti, M. Volatier-Ravat, V. Aimez, G. A. Siviloglou, and D. N. Christodoulides, Phys. Rev. Lett. **103**, 093902 (2009).
[30] L. Xiao, X. Zhan, Z. H. Bian, K. K. Wang, X. Zhang, X. P. Wang, J. Li, K. Mochizuki, D. Kim, N. Kawakami, W. Yi, H. Obuse, B. C. Sanders, and P. Xue, Nat. Phys. **13**, 1117 (2017).
[31] L. Xiao, K. Wang, X. Zhan, Z. Bian, K. Kawabata, M. Ueda, W. Yi, and P. Xue, Phys. Rev. Lett. **123**, 230401 (2019).
[32] J. Li, A. K. Harter, J. Liu, L. de Melo, Y. N. Joglekar, and L. Luo, Nat. Commun. **10**, 855 (2019).
[33] Y. Jiang, Y. Mei, Y. Zuo, Y. Zhai, J. Li, J. Wen, and S. Du, Phys. Rev. Lett. **123**, 193604 (2019).

[34] Y. Wu, W. Liu, J. Geng, X. Song, X. Ye, C.-K. Duan, X. Rong, and J. Du, Science **364**, 878 (2019).
[35] W. Liu, Y. Wu, C.-K. Duan, X. Rong, and J. Du, arXiv:2002.06798.
[36] M. Naghiloo, M. Abbasi, Y. N. Joglekar, and K. W. Murch, Nat. Phys. **15**, 1232 (2019).
[37] M. Partanen, J. Goetz, K. Y. Tan, K. Kohvakka, V. Sevriuk, R. E. Lake, R. Kokkoniemi, J. Ikonen, D. Hazra, A. Mäkinen, E. Hyyppä, L. Grönberg, V. Vesterinen, M. Silveri, and M. Möttönen, Phys. Rev. B **100**, 134505 (2019).
[38] F. Klauck, L. Teuber, M. Ornigotti, M. Heinrich, S. Scheel, and A. Szameit, Nat. Photonics **13**, 883 (2019).
[39] W.-C. Wang, Y.-L. Zhou, H.-L. Zhang, J. Zhang, M.-C. Zhang, Y. Xie, C.-W. Wu, T. Chen, B.-Q. Ou, W. Wu, H. Jing, and P.-X. Chen, arXiv:2006.16467 [Phys. Rev. Lett. (to be published)].
[40] D. Leibfried, D. M. Meekhof, B. E. King, C. Monroe, W. M. Itano, and D. J. Wineland, Phys. Rev. Lett. **77**, 4281 (1996).
[41] See Supplemental Material at http://link.aps.org/supplemental/10.1103/PhysRevLett.126.083604 for further details about experimental setup, data analysis, and theoretical treatment, which includes Refs. [42–45].
[42] C. D. Bruzewicz, J. Chiaverini, R. McConnell, and J. M. Sage, Appl. Phys. Rev. **6**, 021314 (2019).
[43] G. Floquet, Ann. Sci. de l'Ecole Norm. Superieure **12**, 47 (1883).
[44] J. H. Shirley, Phys. Rev. **138**, B979 (1965).
[45] H. Sambe, Phys. Rev. A **7**, 2203 (1973).
[46] D. C. Brody and E.-M. Graefe, Phys. Rev. Lett. **109**, 230405 (2012).
[47] X. Luo, J. Huang, H. Zhong, X. Qin, Q. Xie, Y. S. Kivshar, and C. Lee, Phys. Rev. Lett. **110**, 243902 (2013).
[48] T. E. Lee and Y. N. Joglekar, Phys. Rev. A **92**, 042103 (2015).
[49] A. K. Harter and Y. N. Joglekar, arXiv:2008.01811.
[50] Y. N. Joglekar, R. Marathe, P. Durganandini, and R. K. Pathak, Phys. Rev. A **90**, 040101(R) (2014).